Available online at www.sciencedirect.com

ScienceDirect

Geochimica et Cosmochimica Acta 126 (2014) 1–17

Geochimica et Cosmochimica Acta

www.elsevier.com/locate/gca

Radiocarbon signatures and size–age–composition relationships of major organic matter pools within a unique California upwelling system

B.D. Walker [a,*], T.P. Guilderson [a,b], K.M. Okimura [a,1], M.B. Peacock [a], M.D. McCarthy [a]

[a] University of California, Santa Cruz, Department of Ocean Science, 1156 High St., Santa Cruz, CA 95064, USA
[b] Lawrence Livermore National Laboratory, Center for Accelerator Mass Spectrometry (CAMS), LLNL-L397, 7000 East Ave., Livermore, CA 94551, USA

Received 9 March 2013; accepted in revised form 23 October 2013; Available online 9 November 2013

Abstract

Coastal upwelling zones are among the most productive regions in the world and play a major role in the global carbon cycle. Radiocarbon (as $\Delta^{14}C$) is a powerful tool for tracing the source and fate of suspended particulate and dissolved organic matter (POM, DOM), and has the potential to reconcile key carbon budgets within upwelling systems. However, the extent to which upwelling processes influence the $\Delta^{14}C$ signature of surface DIC, or that of POM or DOM remains almost completely unknown. Here we present a time series of stable carbon ($\delta^{13}C$) and $\Delta^{14}C$ isotopic data of major water column carbon pools, including dissolved inorganic carbon (DIC), large (0.7–500 μm) and small (0.1–100 μm) POM, and high molecular weight (HMW; ~1 nm–0.1 μm) DOM from an upwelling center along the Big Sur coast. We show that DIC $\Delta^{14}C$ values (ranging between +29‰ and −14‰) are strongly correlated to coastal upwelling processes, and that this ^{14}C-signal readily propagates into both the POM and HMW DOM pool. However, the presence of negative POM and HMW DOM $\Delta^{14}C$ values (ranging between +46‰ and −56‰, +6‰ and −123‰ and −1‰ and −150‰, respectively) suggests contributions of "pre-aged" OM, complicating the direct use of "bulk" $\Delta^{14}C$ for tracing upwelling-derived carbon production/export. Using a triple-isotope mixing model ($\delta^{13}C$, $\delta^{15}N$, $\Delta^{14}C$) we estimate that 50–90% and 45–51% of large and small POM is newly-produced OM, while between 6–22% and 12–44% of large and small POM are derived from "pre-aged" re-suspended sediments. Finally, we observe quantitative relationships between OM size, composition (C:N ratio) and $\Delta^{14}C$ within this upwelling system, possibly representing a new tool for modeling ocean C and N biogeochemical cycles.

1. INTRODUCTION

Coastal upwelling regions are among the most dynamic and important components of the ocean carbon cycle. While they make up only about 1% of ocean surface area, they are responsible for >10% of global new production (Chavez, 1995). More recent export production estimates suggest that these regions could be responsible for >40% of all ocean carbon sequestration in the modern ocean (Muller-Karger et al., 2005). As part of the California Current System (CCS), the Big Sur coast is located at the center of a globally significant upwelling region. Recent pCO_2 measurements and models suggest sea-to-air degassing of upwelled CO_2 is greatly attenuated by biological activity and that a major fraction of margin-derived dissolved and particulate organic matter (DOM, POM) may be exported from continental margins

* Corresponding author. Present address: University of California, Irvine, Department of Earth System Science, 3200 Croul Hall, Irvine, CA 92697-3100, USA. Tel.: +1 949 824 8794; fax: +1 949 824 3874.
E-mail address: brett.walker@uci.edu (B.D. Walker).
[1] Present address: San Francisco State University, Romberg Tiburon Center for Environmental Research, 3152 Paradise Drive, Tiburon, CA 94920, USA.

0016-7037/$ - see front matter © 2013 Elsevier Ltd. All rights reserved.
http://dx.doi.org/10.1016/j.gca.2013.10.039

to open ocean environments (Barth et al., 2002; Hales et al., 2005; Gruber, 2006; Pennington et al., 2010). The overall balance of OM flux in the CCS (i.e. local burial vs. export), thus represents a dramatic example of a system in which physical and biogeochemical cycles are inexorably linked (Collins et al., 2003).

Tracing and quantifying the fate of OM produced within upwelling systems has proven to be a difficult task. Most studies seeking to reconcile coastal upwelling carbon budgets involve sampling of multiple carbon reservoirs coupled with total organic carbon (TOC) measurements, in order to reconstruct overall carbon balance using physical transport models (Pennington et al., 2010). However, a major complication to this approach is that TOC measurements are not source-specific and cannot directly trace 'upwelling-derived' OM production or ultimate carbon sources. Together, these limitations substantially complicate efforts to quantitatively understand upwelling system carbon budgets. In contrast, radiocarbon (as $\Delta^{14}C$) is a highly specific tracer for the source and turnover of OM (e.g. McNichol and Aluwihare, 2007 and references therein), that may have particularly powerful applicability to upwelling systems. Because recently upwelled water masses are oversaturated in dissolved inorganic carbon (DIC) that carries a negative $\Delta^{14}C$ signature relative to surface DIC and $CO_{2\ atm}$, $\Delta^{14}C$ values may act as a *direct* tracer of upwelled DIC into primary production, and its subsequent fate within major marine OM reservoirs.

To date, the few studies that have compared $\Delta^{14}C$ measurements in relation to upwelling processes have confirmed the validity of this approach. Robinson (1981) observed a strong correlation between DIC and mussel tissue $\Delta^{14}C$ to the Bakun upwelling index, and found that upwelling of DIC (with >100‰ range in $\Delta^{14}C$ values) was a more conservative indicator of upwelling processes than temperature, salinity or nutrient content (Bakun, 1973; Robinson, 1981). Smaller DIC $\Delta^{14}C$ seasonal offsets (~8–14‰) have also recently been observed for the Southern California Bight – also significantly correlated to upwelling strength (Hinger et al., 2010; Santos et al., 2011). In addition, seasonal variations in surface water DIC and POM $\Delta^{14}C$ (up to 53‰) were observed at Station M on the offshore edge of the CCS in 1991–1996 (Druffel et al., 1996; Masiello et al., 1998). Finally, Rau et al. (2001b) found a strong correlation between the monthly averaged upwelling index and the $\Delta^{14}C$-content of juvenile rockfish during 1995–1997, indicating that upwelled DIC $\Delta^{14}C$ can rapidly propagate from the base of the food web to trophic levels ~3–4. Together, these studies suggest that $\Delta^{14}C$ is a powerful tool for examining the source-specific incorporation of upwelling-derived carbon into major OM pools.

One possible complication for applying this approach is the continued dilution of the "bomb" atmospheric $^{14}CO_2$ signal. Originally introduced in the 1950s and 1960s during atmospheric thermonuclear weapons testing, atmospheric and upper ocean ^{14}C levels have been declining steadily (~4‰ per year in surface Pacific Ocean; Mahadevan, 2001). While estimates of DIC $\Delta^{14}C$ gradients from the surface mixed-layer in the early 1990s were on the order of ~100‰ (Key et al., 1996), today this offset is expected to be much smaller. However, the actual magnitude of a potential coastal DIC $\Delta^{14}C$ offset would also result from multiple oceanographic factors, including: surface ocean DIC $\Delta^{14}C$ gradients, $\Delta^{14}C$ of nearshore sources and mixing, and the intensity and average depth of coastally upwelled DIC $\Delta^{14}C$.

A major goal of this study is to determine whether or not a measurable $\Delta^{14}C$ offset exists within interseasonal *in situ* DIC on the central CA coast – one large enough to be useful as an upwelling tracer. In addition, because OM size is strongly linked to both physical transport and fate (sinking vs. advection, relative sinking rate as well as bioavailability), a second major goal of this study is to evaluate how an upwelled $\Delta^{14}C$-signal propagates into size-fractionated DOM and POM pools. Here, we isolated POM as large (0.7–500 μm) and small (0.1–100 μm) size fractions, and high molecular weight DOM (HMW; 1 nm–0.1 μm) via ultrafiltration. Variations in stable carbon ($\delta^{13}C$) and $\Delta^{14}C$ isotopic signatures of these OM pools and *in situ* DIC are evaluated, throughout a 1.5 yr time series on the Big Sur coast. We evaluate contributions of "pre-aged" (^{14}C-depleted) OM to these size-fractionated OM pools and discuss observed OM size, ^{14}C-age and composition (C:N molar ratio) relationships. To the best of our knowledge, this study represents the first contemporaneous examination of $\delta^{13}C$ and $\Delta^{14}C$ seasonal variability of DIC, HMW DOM and POM size fractions from the CCS.

2. METHODS

2.1. Study site

Biweekly seawater samples were collected from September 2007 to April 2009 at the Granite Canyon Marine Pollution Studies Laboratory (GCMPSL) on the Big Sur coast (Fig. 1). The GCMPSL is an active Scripps Institution of Oceanography (SIO) Shore Station program monitoring site and boasts a >40 year record of sea surface temperature (SST) and salinity data from a unique high nutrient, low-chlorophyll (HNLC) region of the central California coast (Hutchins and Bruland, 1998; Hutchins et al., 1998; Bruland et al., 2001; Biller et al., 2013). In addition, seawater sampled from the GCMPSL has been previously shown to be highly representative of CCS waters (Breaker, 2005; Walker and McCarthy, 2012). In particular Walker and McCarthy (2012) show that seawater physical properties (SST, salinity, sigma-*t*), nutrients (nitrate, ammonium, phosphate, silicic acid) and major organic matter pools (DOM, POM) are biogeochemically and isotopically representative of the CCS during three main oceanographic periods. In this study, we described these as: (1) the "Oceanic 2007" period, from mid-September to mid-October 2007, (2) the winter "Davidson 2007" period, from mid-October 2007 to early-March 2008, (3) the spring/summer "Upwelling 2008" period, from mid-March to early-July 2008, (4) the "Oceanic 2008" period from late-July to mid-October 2008 and (5) the "Davidson 2008" period, from late-November 2008 to mid-March 2009 (Walker and McCarthy, 2012). Finally, contemporaneous sample comparisons between the GCMPSL seawater intake system

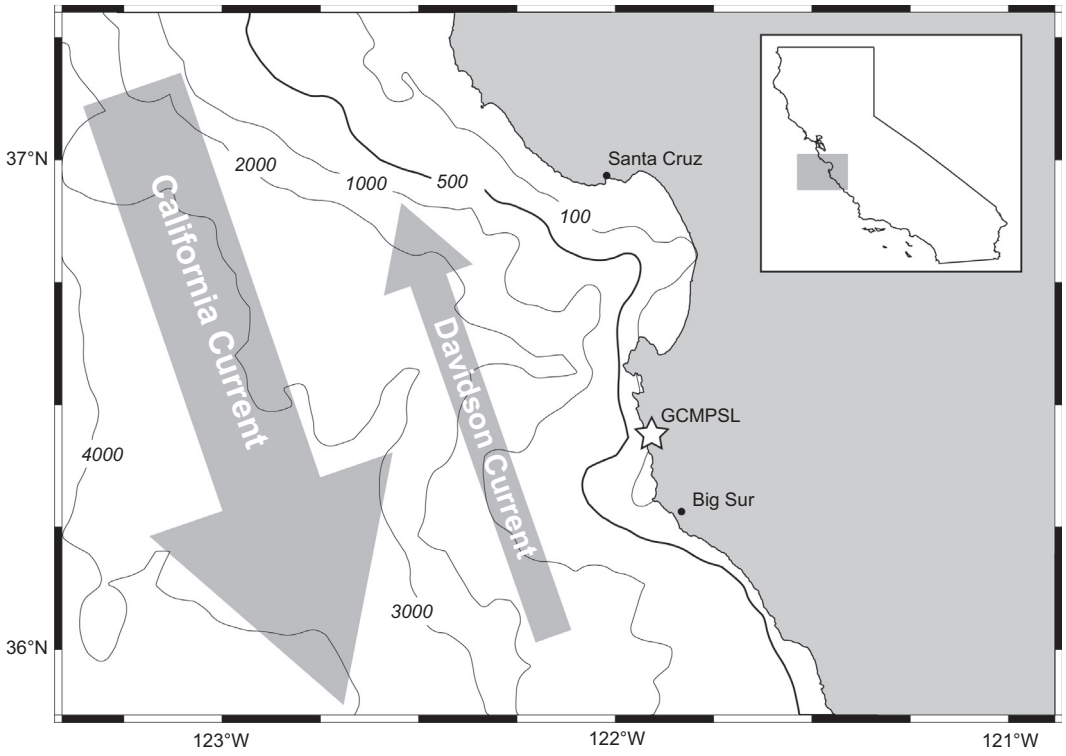

Fig. 1. Study site: The Granite Canyon Marine Pollution Studies Laboratory (GCMPSL) is located adjacent to the Monterey Bay on the Central Coast of California. Inlayed map shows the relative location of the Monterey Bay area with respect to the California coastline with bathymetric contours (black lines) and major CCS ocean currents (large grey arrows). Note the narrow shelf directly offshore GCMPSL and along the Big Sur Coast.

and the adjacent channel (this study) were statistically indistinguishable in nutrient concentrations, OM content, $\Delta^{14}C$ and $\delta^{13}C$ isotopic signatures.

2.2. Dissolved and particulate sample collection

DIC samples were collected in 7.4 ml (2 dram) vials from 0.7 μm (Whatman GF/F) filtrates, and preserved with 20 μl of a saturated $HgCl_2$ solution, filled to zero headspace and stored with Parafilm-M® sealed caps at 4 °C until sample analysis. All glassware and filters were combusted (450 °C/4 h) prior to sample collection. Detailed DOM and POM sampling protocols have been previously described (Walker and McCarthy, 2012). Briefly, HMW DOM samples (HMW DOM: 1 nm–0.1 μm) were collected via a homebuilt ultrafiltration system using GE Osmonics membranes (NMWCO = 2.5 kDa, model # GE2540-F1072; Walker et al., 2011; Walker and McCarthy, 2012). Seawater volumes of ~1500–2000 L were used for all HMW DOM isolates, and each were concentrated to 2 L in the field, and frozen until de-salted via diafiltration with 20 L 18.2 MΩ Milli-Q water in the lab. After diafiltration, HMW DOM samples were dried via centrifugal evaporation, homogenized with a mortar and pestle and stored in pre-combusted (450 °C/4 h) vials in a desiccators prior to isotopic analyses.

Large (~0.7–500 μm) POM size-fraction samples were collected onto Whatman GF/F filters for stable isotopic analysis and Whatman QMA quartz filters for $\Delta^{14}C$ analysis. Small POM samples (0.1–100 μm) were collected from pre-filtered seawater (<100 μm) using a homebuilt system equipped with a hollow-fiber membrane (Amersham Biosciences, model # CFP-1-E-55; Roland et al., 2009). These ultrafiltered suspended POM (UPOM) samples were reduced to ~2 L and diafiltered in the field, then dried via centrifugal evaporation, homogenized with a mortar and pestle and stored in pre-combusted vials in a desiccator prior to isotopic analyses.

2.3. Carbon isotopic analysis

2.3.1. DIC $\delta^{13}C$ analysis

Carbon isotopic ($\delta^{13}C$) analysis of DIC samples was performed at the University of California, Santa Cruz (UCSC) Stable Isotope Laboratory (SIL) using a Thermo-Scientific Gas Bench II interface coupled to a ThermoFinningan Delta Plus XP isotope ratio mass spectrometer (IRMS) following methods similar to Torres et al. (2005). Seawater DIC samples were injected (1.0 mL) into helium flushed 12 mL Exetainer® vials containing 1 mL of 43% phosphoric acid. Over a period of greater than 6 h, DIC derived CO_2 was allowed to evolve from the acidified water into the headspace. After this equilibration period, the headspace gas was entrained into a He stream, passed through two Nafion dryers and passed through a PoraPlot Q gas chromatographic

(GC) column to purify CO_2 from N_2O gas. During analysis, calibrated in-house $NaHCO_3$ standards were interspersed between samples to correct for linearity (size) effects and drift. A second calibrated internal laboratory standard was also run to monitor quality control. Standards were prepared daily by dissolving $NaHCO_3$ bulk powders in water previously stripped of DIC by sonicating under a weak vacuum for 1 h. These laboratory standards were calibrated against NIST Standard Reference Materials (NBS-19, NBS-18, and LSVEC). Corrected delta values are expressed relative to V-PDB (Vienna Pee-Dee Belemnite) scale for $\delta^{13}C$ (‰). Average external precision of DIC concentrations and $\delta^{13}C$ measurement based on sample duplicates were ±0.1 mmol/kg and ±0.04‰, respectively.

2.3.2. Organic matter isotopic analysis

Stable isotopic analysis for organic matter samples were performed at the UCSC SIL by CHN analysis using a Carlo Erba CHNO-S EA-1108 Elemental Analyzer and Thermo-Finnigan Delta Plus XP isotope ratio mass spectrometer (Fry et al., 1992). Analytical precision of internationally calibrated in-house standards was better than 0.2‰ for both $\delta^{13}C$ matter. Sample isotopic values are corrected for size, drift and source stretching effects. Carbon and nitrogen elemental composition is estimated based on standards of known elemental composition. POM GF/F and QMA filters were dried overnight in an oven at 40 °C, then vapor acidified (12 N HCl, 12 hr) and dried again prior to CHN and $\Delta^{14}C$ analysis. Small POM and HMW DOM samples were directly acidified with 1 N HCl in either silver capsules or pre-combusted (450 °C/4 hr) quartz tubes to remove residual carbonates and oven dried (40 °C) overnight prior to CHN analysis. Results are reported in standard per mil (‰) notation and relative to V-PDB for $\delta^{13}C$. Average external precision for $\delta^{13}C$ (based on $n = 3$ sample replicates) was ±0.3‰.

2.3.3. Radiocarbon analysis and AMS measurement

Natural abundance radiocarbon ($\Delta^{14}C$) measurements were performed at both the Center for Accelerator Mass Spectrometry at Lawrence Livermore National Laboratory (CAMS/LLNL) or at the National Ocean Science Accelerator Mass Spectrometry (NOSAMS) Facility at Woods Hole Oceanographic Institution (WHOI) following standard graphitization procedures (Vogel et al., 1987). The isolation of DIC from seawater samples for $\Delta^{14}C$ analysis was performed by vacuum line extraction at UC Davis Department of Geological Sciences, following methods established for the extraction of ΣCO_2 from seawater (McNichol et al., 1994). Large and small POM size fractions and HMW DOM samples were converted to CO_2 gas by closed tube combustion. Results are reported as age-corrected $\Delta^{14}C$ (‰) for geochemical samples and have been corrected to the date of collection and are reported in accordance with conventions set forth by Stuiver and Polach (1977). Isotopic $\Delta^{14}C$ results are reported as Fraction Modern (FM), $\Delta^{14}C$, and conventional radiocarbon age (ybp).

2.4. Estimation of POM source contributions using MixSIR

We used MixSIR v.1.0.4 (Moore and Semmens, 2008) to determine the relative contributions of multiple OM sources to both large and small POM size fractions. MixSIR uses a Bayesian framework to generate probability distributions that incorporate multiple isotopes and multiple sources of uncertainty. Model inputs included mean and standard deviation values for potential POM source contributions and also individual size-fractionated POM data in three isotopic dimensions ($\delta^{13}C$, $\delta^{15}N$, $\Delta^{14}C$). We assume no fractionation factors (trophic enrichment, etc.) between source and resulting mixture values for any of the three isotopes. MixSIR model outputs are reported as the contribution of each source endmember to the mixture at the median (50%) level of the distribution. Percent standard deviations (SD) for each source contribution was determined using the relationship between SD and the interquartile range (IQR = 75–25% interval of the distribution): SD = IQR/1.35. In all models, we used uninformative priors (i.e. no weighted importance of source contributions), and 1×10^8 iterations such that recommended thresholds for generating robust maximum likelihoods of the posterior distributions were met without posterior draws.

3. RESULTS AND DISCUSSION

3.1. Dissolved inorganic carbon $\Delta^{14}C$ and $\delta^{13}C$ signatures: physical and biological coupling

A primary goal of this study is to evaluate the current $\Delta^{14}C$ offset of DIC and its linkage to physical processes within an upwelling system. Very few studies have presented DIC $\delta^{13}C$ signatures for upwelling regions (e.g. Rau et al., 2001a), however DIC $\delta^{13}C$ signatures from both the open ocean and the outer CCS have strong depth trends (ranging from ~+2‰ in surface to −0.5‰ at depth; WOCE Leg P17N, Stations #6,10,39; Masiello et al., 1998, Station M). This suggests that a direct relationship would also be expected between DIC $\delta^{13}C$ and regional upwelling at this site (Breaker, 2005; Walker and McCarthy, 2012). However, several studies have also observed significant biological fractionation of *in situ* DIC $\delta^{13}C$ via: (1) direct uptake of HCO_3^- (2) passive diffusion or active uptake of $CO_{2\,aq}$ or (3) equilibration of $CO_{2\,aq}$ with the atmosphere (Rau et al., 1997b, 2001a; Laws et al., 2002; Cassar et al., 2004). A decoupling of DIC $\delta^{13}C$ signatures from physical forcing would generally imply that biological processes largely influence DIC isotopic fractionation. However, because linkages to physical forcing underlies much of the isotopic data, we first evaluate correlations between DIC concentrations, $\delta^{13}C$ and $\Delta^{14}C$ signatures to physical and biological processes.

3.1.1. DIC $\Delta^{14}C$ seasonal trends and offsets

Average measured DIC $\Delta^{14}C$ values (average = +11 ± 13‰, $n = 30$) were significantly lower than surface ocean $\Delta^{14}C$ values previously reported for the North Eastern Pacific (NEP; +68 ± 20‰; Masiello et al.,

1998). We observed a large seasonal trend in DIC $\Delta^{14}C$ signatures with the most negative $\Delta^{14}C$ values ($-5 \pm 7‰$, $n = 9$) during spring/summer upwelling (March–July, 2008) and the most positive $\Delta^{14}C$ values ($+18 \pm 7‰$, $n = 21$) during summer/fall "Oceanic" (July–October) and winter "Davidson" (November–February) periods (Table 1 and Fig. 2). We observed a total DIC $\Delta^{14}C$ seasonal range of ~43‰ ($\Delta^{14}C = -14‰$ to $+29‰$). This $\Delta^{14}C$ offset is similar to $\Delta^{14}C$ offsets reported from 25 and 85 m depths in the NEP (33‰ and 53‰, respectively; Masiello et al., 1998). DIC $\Delta^{14}C$ signatures were tightly correlated with water mass properties. Statistically significant correlations were observed between DIC $\Delta^{14}C$ vs. previously reported density (σ_t), sea surface temperature (SST) and salinity ($R^2 \geqslant 0.62$, $p < 0.0001$; Walker and McCarthy, 2012). This correlation is also consistent with expected trends in the open ocean. In fact, we found a virtually identical correlation ($R^2 = 0.69$, $p < 0.0001$) by regressing all WOCE (P17N) DIC $\Delta^{14}C$ and temperature data for samples taken from above 200 m depth. Our measured DIC $\Delta^{14}C$ were also

Table 1
Dissolved inorganic carbon: stable and radiocarbon isotopic data. This table summarizes all dissolved inorganic carbon (DIC) concentration (mmol/kg) and isotopic ($\delta^{13}C$ and $\Delta^{14}C$) data. Errors given for $\delta^{13}C$ data (‰) represent the 1σ standard deviation at least $n = 3$ analyses. Where more than one CAMS# is present, the $\Delta^{14}C$ error represents half of the range between two independent sample measurements.

Sample date	DIC (mmol kg^{-1})	DIC $\delta^{13}C$ (‰)	±	CAMS #	Fm	±	$\Delta^{14}C$ (‰)	±	^{14}C age	±
09/20/03	n.d.	n.d.		n.d.						
09/21/03	n.d.	n.d.		n.d.						
09/22/03	n.d.	n.d.		n.d.						
09/23/03	n.d.	n.d.		n.d.						
09/24/03	n.d.	n.d.		n.d.						
10/08/03	2.60	−0.32	0.06	138810	1.021	0.005	21	4.8	>Modern	
11/11/03	2.27	0.14	0.09	143184	1.027	0.005	20	5.4	>Modern	
11/26/03	2.31	0.01		138811	1.025	0.005	25	4.6	>Modern	
12/13/03	2.42	0.02	0.06	143180	1.026	0.005	18	4.7	>Modern	
01/15/04	2.55	0.10		143190	1.027	0.004	19	4.1	>Modern	
01/28/04	2.36	0.38	0.02	143457	1.024	0.006	17	5.7	>Modern	
02/11/04	2.30	−0.06	0.01	143187	1.031	0.004	24	4.1	>Modern	
02/28/04	2.32	0.23	0.05	143168	1.023	0.004	15	4.0	>Modern	
02/29/04	2.36	0.22	0.01	138812	1.023	0.006	23	5.9	>Modern	
03/01/04	2.35	0.02	0.04	143173	1.027	0.004	20	4.1	>Modern	
03/17/04	2.50	−0.34	0.05	138813	0.986	0.005	−14	4.6	Modern	
03/31/04	2.32	0.12		143185	1.010	0.005	2	4.7	Modern	
04/13/04	2.16	−0.05		143170	1.012	0.004	5	4.4	>Modern	
04/27/04	2.07	0.03		143177	1.006	0.004	−1	4.0	Modern	
05/08/04	n.d.	0.00		143188	0.998	0.004	−9	3.9	Modern	
05/09/04	2.02	−0.10		143183	0.993	0.004	−14	3.9	Modern	
05/10/04	2.23	−0.11		143172	1.000	0.004	−7	3.8	Modern	
05/27/04	1.75	0.38		143174	1.012	0.004	5	4.1	Modern	
06/11/04	1.91	0.18		143169	1.009	0.004	2	4.1	Modern	
06/11/04				*143458*[†]	*0.987*	*0.005*	*−20*	*4.6*	*Modern*	
06/26/04	1.83	0.48		n.d.						
07/08/04	1.91	0.32		143176	1.012	0.004	5	4.0	Modern	
07/22/04	1.88	0.05	0.03	143171	1.008	0.004	1	4.0	Modern	
08/05/04	1.95	0.03		143186/143459	1.015	0.005	8	0.5	>Modern	
08/20/04	1.89	0.51		143189	1.036	0.004	29	4.2	>Modern	
09/11/04	1.95	0.58	0.05	143182	1.035	0.004	27	4.2	>Modern	
09/12/04	1.82	0.44		143191	1.028	0.004	21	4.2	>Modern	
09/13/04	1.85	0.43		n.d.						
09/14/04	2.24	0.44		143179	1.028	0.004	20	4.3	>Modern	
09/22/04	1.80	0.43		143456	1.016	0.004	9	4.5	Modern	
09/23/04	1.87	0.20		143181	1.026	0.004	19	4.1	>Modern	
10/17/04	1.90	0.40		143178	1.027	0.005	20	4.9	>Modern	
11/25/04	1.82	0.66		143175	1.028	0.004	21	4.2	>Modern	
12/16/04	n.d.	n.d.		n.d.						
1/15/2009T	n.d.	n.d.		n.d.						
1/15/2009C	n.d.	n.d.		n.d.						
02/04/05	n.d.	n.d.		n.d.						
02/09/05	n.d.	n.d.		n.d.						
02/25/05	n.d.	n.d.		n.d.						
03/09/05	n.d.	n.d.		n.d.						

[†] We consider the replicate analysis of 6/12/08 DIC sample (CAMS#143458) to be an outlier, falling nearly outside 3σ the DIC $\Delta^{14}C$ population mean of $+10.7 \pm 13.4‰$. All other DIC $\Delta^{14}C$ values fall within 2σ the population mean.

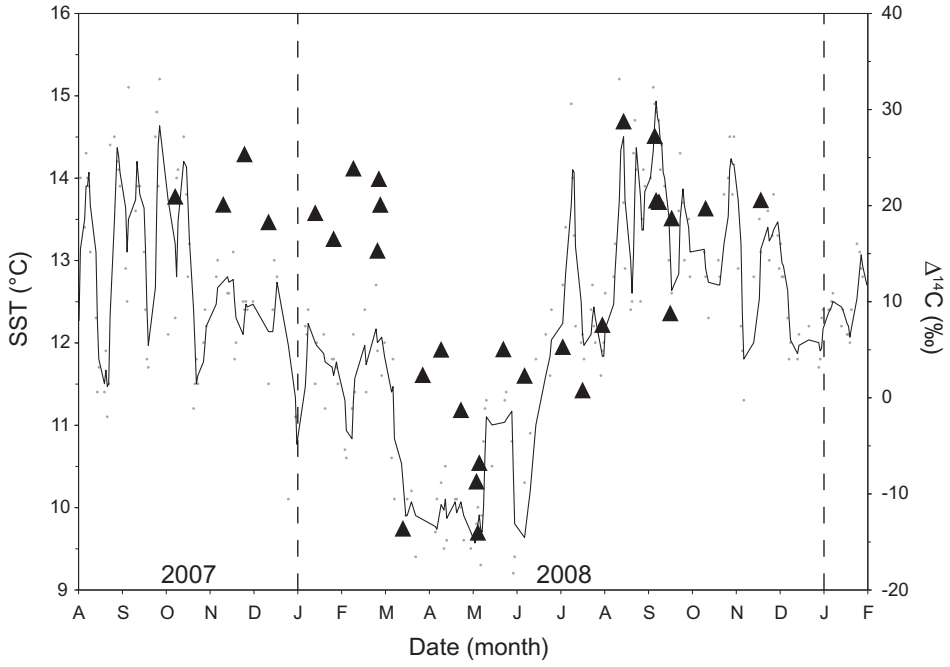

Fig. 2. Dissolved inorganic carbon (DIC) $\Delta^{14}C$ signatures. DIC $\Delta^{14}C$ values (solid triangles; right *y*-axis) show a large seasonal offset due to variable upwelling within the Granite Canyon upwelling system. Data is shown for day sampled (September 2007–January 2009). The solid line represents the 3-day moving average in Sea surface temperature (SST in °C). Grey dots are daily SST data taken as part of the SIO Shore Stations program (data available from http://shorestation.ucsd.edu/).

correlated to the 3-day average upwelling index ($R^2 = 0.34$, $p = 0.0007$; NBDC #46042).

These results are in agreement with work suggesting wind-driven mixing and advection (as opposed to organic matter remineralization or atmospheric gas exchange processes) are main drivers for DIC $\Delta^{14}C$ variability within the CCS (Masiello et al., 1998). It should also be noted that because $\Delta^{14}C$ values are normalized for biological fractionation ($\delta^{13}C$), photosynthetic processes and the associated isotopic fractionation do not influence our reported $\Delta^{14}C$ signatures. The specific $\Delta^{14}C$ offsets observed through a seasonal upwelling cycle further indicate that within this central CA upwelling region of the CCS, physical forcing and the upwelling of deeper CCS water results in a DIC $\Delta^{14}C$ offset of ~40‰. The similarity of this offset with that observed in the early 1990s might at first seem unexpected; this offset is driven not only by $^{14}CO_{2\,atm}$ concentrations, but also by relative local intensity of coastal upwelling (i.e. the presence of a more negative $\Delta^{14}C$ DIC-endmember). The variability is sufficient (~10 times greater than $\Delta^{14}C$ analytical error) to be used as an effective geochemical tracer in upwelling systems.

3.1.2. DIC concentration and $\delta^{13}C$: seasonal trends and biological linkages

In upwelling systems, both physical (mixing, degassing) and biological (phytoplankton active HCO_3^- uptake or passive diffusion) processes influence DIC concentrations and $\delta^{13}C$ values (Tortell et al., 2000; Rau et al., 2001a; Hales et al., 2005; Fassbender et al., 2011). Here we evaluate the effect of biological processes in determining DIC concentrations and $\delta^{13}C$ signatures in this upwelling system. We observed variability in DIC concentrations (~1.7–2.6 mmol/kg) and $\delta^{13}C$ signatures (−0.34‰ to +0.66‰; Table 1). While measured DIC $\delta^{13}C$ values were significantly correlated to SST, salinity, σ_t and upwelling index ($R^2 \geqslant 0.34$, $p \leqslant 0.0007$; Fig. 3A), DIC concentrations were not significantly correlated to any of these seawater properties ($p \geqslant 0.15$). This result is somewhat unexpected given that NCP DIC concentrations profiles generally correlated to temperature and salinity (e.g. WOCE P17N, <200 m; $R^2 = 0.60$, $p \leqslant 0.0001$ and $R^2 = 0.16$, $p = 0.0442$). The relationship between our DIC $\delta^{13}C$ and nitrate concentrations (Fig. 3B; $R^2 = 0.42$, $p < 0.0001$) suggests that biological processes exert a primary control on the DIC pool at this site. Both DIC concentration and $\delta^{13}C$ values are also significantly correlated to POM $\delta^{13}C$ values (Fig. 3C and D). This observation is consistent with the idea that DIC $\delta^{13}C$ signatures will fractionate during bicarbonate and/or CO_2 uptake by coastal phytoplankton and also with strong correlations previously observed between DIC concentrations and $\delta^{13}C$ vs. POC and PON ($R^2 \geqslant 0.59$, $p < 0.0001$ and $R^2 \geqslant 0.0.36$, $p \leqslant 0.0005$ for DIC $\delta^{13}C$ and DIC concentration, respectively; Walker and McCarthy, 2012). These observations agree with recent research showing that primary production can have an appreciable effect on DIC within upwelling systems – capable of reducing DIC by ~200 μmol/kg in ~10 days (e.g. Fassbender et al., 2011). Changes in pCO_2 and DIC concentrations have also been previously shown to have an appreciable effect on DIC $\delta^{13}C$ signatures within coastal and open ocean ecosystems

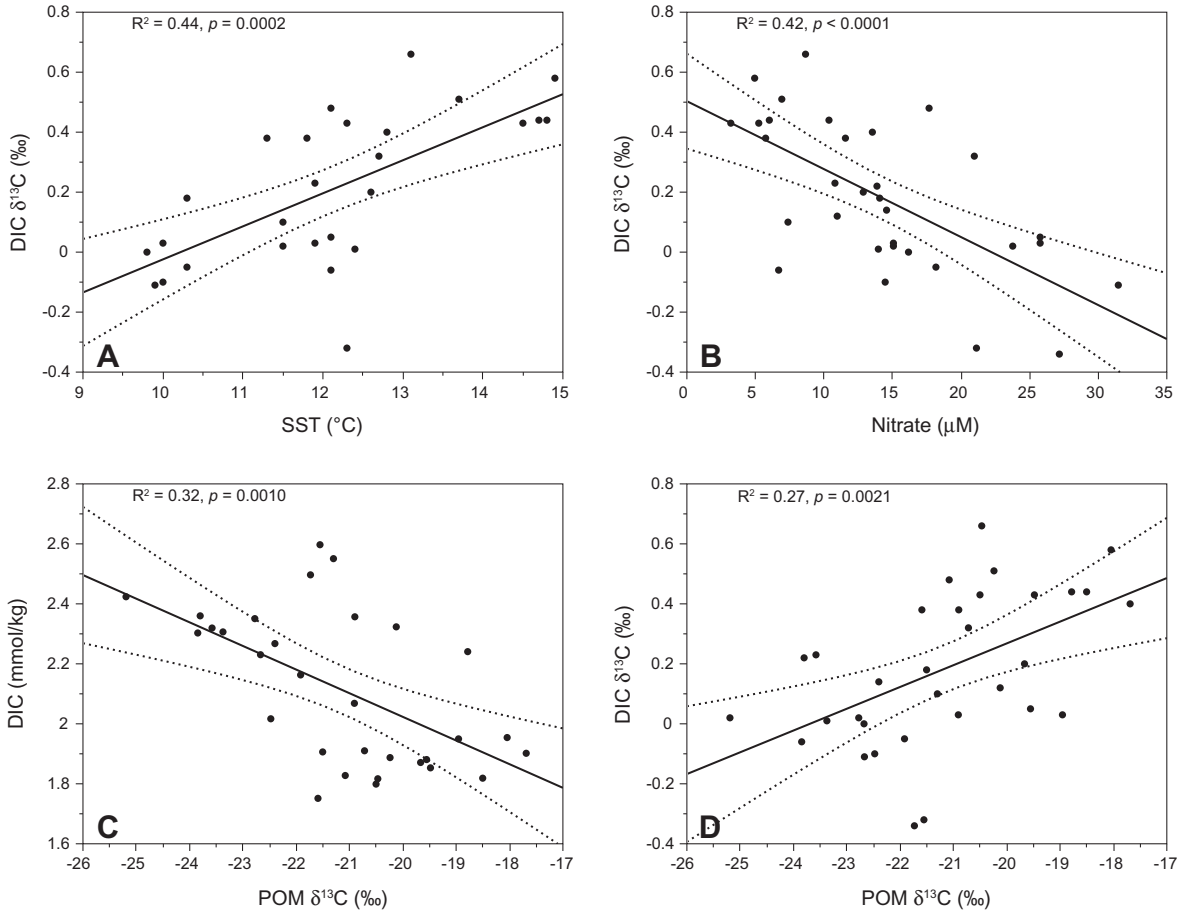

Fig. 3. DIC concentration and $\delta^{13}C$ shows influence of physical and biological processes. Least squares regression analysis is shown for: (A) Dissolved inorganic carbon (DIC) $\delta^{13}C$ signatures (‰) vs. sea surface temperature (SST). (B) DIC $\delta^{13}C$ vs. nitrate concentration (C) DIC concentrations (mmol/kg) vs. large POM $\delta^{13}C$. (D) DIC $\delta^{13}C$ vs. large POM $\delta^{13}C$. For all plots, thick black lines and dashed lines represent the linear fit and 95% confidence limits.

(Rau et al., 1989, 1997a,b, 2001a). The apparent decoupling of DIC from physical processes, combined with statistically significant correlations of DIC $\delta^{13}C$ to both the POM pool, indicates that biological processes have a large impact on DIC concentrations and $\delta^{13}C$ signatures within this coastal upwelling system.

3.2. Radiocarbon signatures of organic matter size fractions

3.2.1. Large vs. small POM size fractions

The seasonal upwelling DIC $\Delta^{14}C$ signal together with observations suggesting active DIC uptake by phytoplankton strongly suggest that negative $\Delta^{14}C$-signatures characteristic of upwelling cycles should also be observed in recently produced OM. Here we examine seasonal offsets within large and small POM $\Delta^{14}C$ signatures, and to what extent DIC $\Delta^{14}C$ is incorporated into POM size-fractions. Measured large POM $\Delta^{14}C$ values displayed a considerable seasonal offset, with observed values ranging from $-55‰$ to $+46‰$ (Fig. 4; average $= -15 \pm 25‰$, $n = 33$). While large POM samples had 'younger' ^{14}C-ages (Table 2A; ^{14}C-age $\leqslant 400$ years), most $\Delta^{14}C$ values were lower than measured DIC $\Delta^{14}C$ (Fig. 4). Despite a noticeable seasonal offset, only weak correlations were found between large POM $\Delta^{14}C$ to a 3-day average upwelling index and to DIC $\Delta^{14}C$ ($R^2 = 0.17$, $p = 0.0168$ and $R^2 = 0.16$, $p = 0.0391$, respectively). In addition, no correlations were found between large POM $\Delta^{14}C$ and seawater physical properties (SST, salinity, σ_t; p-values $\geqslant 0.08$) at the 95% confidence interval.

Small POM (UPOM; 0.1–100 μm) $\Delta^{14}C$ values also displayed a large seasonal range ($-123‰$ to $-1‰$; Table 2B). Average small POM $\Delta^{14}C$ values ($\Delta^{14}C = -26 \pm 40‰$, $n = 10$) were slightly lower than the large POM size fraction ($\Delta^{14}C = -15 \pm 25‰$, $n = 33$; Fig. 4), however this difference is not significant (Student's t-test, $p = 0.27$, $\alpha = 0.05$). The late summer "Oceanic" period is the only CCS seasonal period in which small POM had $\Delta^{14}C$ values within DIC $\Delta^{14}C$ ranges. Small POM samples from all other CCS periods (i.e. spring/summer "Upwelling" and winter "Davidson") were highly variable, and had more substantially negative $\Delta^{14}C$ values than DIC. In contrast to large POM, a strong statistical correlation was found between small POM $\Delta^{14}C$ and upwelling index (3-day average; $R^2 = 0.73$, $p = 0.0021$). However, no significant correlations were observed between small POM $\Delta^{14}C$ vs. *in situ*

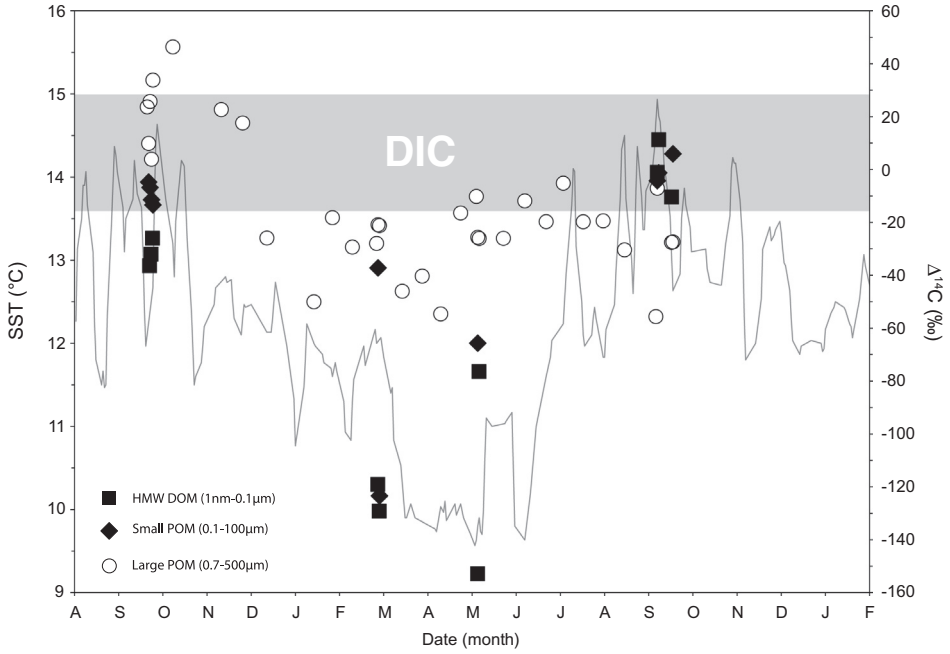

Fig. 4. Radiocarbon signatures of POM and HMW DOM size-fractions. Large and small POM $\Delta^{14}C$ values throughout the time series by date (September 2007–January 2009) are represented by open circles (GFF-POM; 0.7–500 μm) and solid diamonds (UPOM; 0.1–100 μm), respectively. Solid squares show high molecular weight (HMW) DOM (~1 nm–0.1 μm) $\Delta^{14}C$ throughout the time series by date (September 2007–January 2009). The most negative $\Delta^{14}C$ HMW DOM sample, (9/21/2007, $\Delta^{14}C = -222‰$; Table 1) is not shown here so that seasonal $\Delta^{14}C$ offsets can be seen more clearly. Sea surface temperature (SST; grey line, first *y*-axis) represents the 3-day moving average in °C (left *y*-axis). The grey shaded bar represents the total range in surface measured DIC $\Delta^{14}C$ values (−15‰ to +29‰). Error bars are smaller than the data points shown.

DIC $\Delta^{14}C$ ($p = 0.74$) or seawater physical properties (SST, salinity, σ_t; $p \geqslant 0.12$, $\alpha = 0.05$).

The observation that both small and large POM size-fractions approached the observed range of *in situ* DIC $\Delta^{14}C$ over multiple seasonal periods indicates that a substantial portion of suspended POM is comprised of recently fixed photosynthetic material. These results are consistent with previous work documenting a strong linkage between physical processes, DIC $\Delta^{14}C$ and the $\Delta^{14}C$-content of marine biota (Robinson, 1981; Rau et al., 2001b). However, the presence of negative $\Delta^{14}C$ values in the large POM size-fraction was unexpected. Previously reported $\delta^{13}C$ and $\delta^{15}N$ stable isotopic values from this study have indicated that the larger POM fraction is more chemically 'fresh' and generally representative of local phytoplankton production (Walker and McCarthy, 2012). Therefore, the large POM $\Delta^{14}C$ signatures we observe suggest additional ^{14}C-depleted (i.e. "pre-aged") OM, sources contribute to the suspended POM pool. The largest contribution of pre-aged OM occurs during periods of intense coastal upwelling (Fig. 4).

For the smaller POM size-fraction, negative $\Delta^{14}C$ values and a lack of significant correlations to seawater physical properties suggest that contributions of "pre-aged" carbon sources more strongly influence the small POM size fraction. This is consistent with elemental (C:N ratios) and stable isotopic data from other ocean regions, indicating small POM is often more degraded, less labile, and have older ^{14}C-ages. We note, however, that the offset between small and large POM $\Delta^{14}C$ signatures is not constant. This variation implies a complex interplay between the strength and duration of wind and current induced re-suspension on the shelf, and heterogeneous OM $\Delta^{14}C$ source signatures. Overall, $\Delta^{14}C$ signatures for both POM size-fractions seem to support this general idea. The lowest $\Delta^{14}C$ values for both POM size-fractions occurred during spring/summer upwelling, consistent with a larger contribution of upwelled "pre-aged" material. These results suggest that suspended POM with relatively "old" ^{14}C-ages (e.g. POM dominated by re-suspended shelf sediments) may represent a significant source of ^{14}C-depleted OM to the open ocean (Bauer and Druffel, 1998; Hwang and Druffel, 2006; Roland et al., 2008).

3.2.2. High molecular weight DOM $\Delta^{14}C$ values: evaluation of sources, production and export

Previous work has shown that HMW DOM from this upwelling system has a bulk stable isotopic ($\delta^{13}C$, $\delta^{15}N$) and chemical composition (C:N molar ratio) similar to large POM, strongly indicating that primary production is responsible for new HMW DOM produced within this upwelling system (Walker and McCarthy, 2012). Here we explore the relative importance of physical processes (seasonal offsets in $\Delta^{14}C$) vs. biological production (comparison to large and small POM $\Delta^{14}C$) in determining HMW DOM $\Delta^{14}C$ signatures in this coastal upwelling system. Using a two-component model, we also evaluate the 'source' $\Delta^{14}C$ signature of recently produced HMW DOM and discuss

Table 2
Large and small suspended particulate organic matter (POM): stable and radiocarbon isotopic data. (A) Large POM (GFF; 0.7–500 μm) carbon isotopic ($\delta^{13}C$ and $\Delta^{14}C$) data. GFF-POM errors given for $\delta^{13}C$ data (‰) represent the 1σ standard deviation at least $n = 3$ analyses. Radiocarbon results are presented as in Table 1. CAMS # with "OS" designation represent $\Delta^{14}C$ data determined at WHOI/NOSAMS. Sample dates ending in "T" and "C" represent contemporaneous sample comparison between the GCMPSL seawater intake system and the adjacent ocean channel. (B) Small POM (UPOM; 0.1–100 μm) carbon isotopic ($\delta^{13}C$ and $\Delta^{14}C$) data.

Sample date	GFF-POM $\delta^{13}C$ (‰)	±	CAMS #	Fm	±	$\Delta^{14}C$ (‰)	±	^{14}C age	±
(A) Large POM (0.7–500 μm)									
09/20/03	−21.1		n.d.						
09/21/03	−22.5		138826	1.024	0.003	24	3.3	>Modern	
09/22/03	−22.2		n.d.						
09/23/03	−21.1	0.64	143698	1.017	0.003	10	2.7	>Modern	
09/24/03	−20.7		138827/138828	1.026	0.006	26	5.6	>Modern	
10/08/03	−21.6	0.03	138829	1.004	0.003	4	3.0	Modern	
11/11/03	−22.4	0.30	n.d.						
11/26/03	−23.4		143491	1.041	0.004	34	3.6	>Modern	
12/13/03	−25.2		143699	1.054	0.004	46	3.7	>Modern	
01/15/04	−21.3	0.36	143763	1.030	0.004	23	4.4	>Modern	
01/28/04	−20.9		143764	1.025	0.004	18	3.7	>Modern	
02/11/04	−23.8		143765	0.981	0.004	−26	3.8	155	35
02/28/04	−23.6		143768	0.957	0.004	−50	4.0	355	35
02/29/04	−23.8		138830	0.982	0.003	−18	3.5	150	30
03/01/04	−22.8		143492	0.978	0.003	−29	2.9	180	25
03/17/04	−21.7		138831	0.972	0.003	−28	3.5	230	30
03/31/04	−20.1		143493	0.986	0.003	−21	3.0	110	25
04/13/04	−21.9		n.d.						
04/27/04	−20.9		143767	0.986	0.003	−21	3.3	115	30
05/08/04	−22.7		138832	0.954	0.003	−46	3.5	380	30
05/09/04	−22.5		138833	0.960	0.004	−40	4.1	330	35
05/10/04	−22.7		138834	0.945	0.003	−55	3.5	450	30
05/27/04	−21.6		143769	0.991	0.004	−16	3.9	75	35
06/11/04	−21.5		143770	0.997	0.003	−10	2.8	Modern	
06/26/04	−21.1		143771	0.981	0.003	−26	3.4	150	30
07/08/04	−20.7		143494	0.981	0.003	−26	3.4	155	30
07/22/04	−19.6		143772	0.981	0.003	−26	3.4	155	30
08/05/04	−19.0		OS - 77983	0.995	0.005	−12	4.7	40	40
08/20/04	−20.2		143639	0.987	0.003	−20	2.8	105	25
09/11/04	−18.0		143640	1.002	0.003	−5	2.6	Modern	
09/12/04	−18.5		143495	0.987	0.003	−20	3.0	105	25
09/13/04	−19.5		143641	0.988	0.003	−19	3.0	100	25
09/14/04	−18.8		143496	0.977	0.003	−30	3.0	190	25
09/22/04	−20.5		n.d.						
09/23/04	−19.7		143497	0.951	0.003	−56	2.9	400	25
10/17/04	−17.7		143643	1.000	0.003	−7	3.2	Modern	
11/25/04	−20.5		n.d.						
12/16/04	−20.9		n.d.						
1/15/2009T	−21.0		143645	0.979	0.004	−28	4.1	165	35
1/15/2009C	−21.5		143644	0.980	0.003	−27	3.3	165	30
02/04/05	−22.4		n.d.						
02/09/05	−22.7		n.d.						
02/25/05	−22.9		n.d.						
03/09/05	−22.3		n.d.						
Sample date	UPOM $\delta^{13}C$ (‰)	±	CAMS #	Fm	±	$\Delta^{14}C$ (‰)	±	^{14}C age	±
(B) Small POM (0.1–100 μm)									
09/21/03	−21.4	0.17	143498	1.002	0.003	−5	3.5	Modern	
09/22/03	−22.0	0.13	152565	1.001	0.004	−7	3.9	Modern	
09/23/03	−19.8	0.35	152566	0.996	0.003	−11	2.8	Modern	
09/24/03	−20.9	0.30	152567	0.994	0.003	−13	2.9	50	25
02/29/04	−22.5	0.22	143647	0.970	0.003	−37	2.5	245	25
03/01/04	−19.9	0.12	143638	0.883	0.003	−123	2.5	1000	25
05/09/04	−22.0	0.00	OS - 78128	0.941	0.003	−66	3.2	490	25
09/12/04	−17.1	0.24	143648	1.003	0.003	−4	2.9	Modern	
09/13/04	−18.8	0.12	143499	1.006	0.003	−1	3.2	Modern	
09/23/04	−18.6	0.22	152568	1.013	0.004	6	3.79895	>Modern	

the implications of seasonal export of isotopically distinct HMW DOM to the CCS.

Of all OM pools measured, HMW DOM $\Delta^{14}C$ values were on average the lowest (average $\Delta^{14}C = -72 \pm 75‰$, $n = 11$; Table 3), and had the largest range (+12‰ to −150‰; Fig. 4). While the majority of HMW DOM $\Delta^{14}C$ values appear to follow a predictable seasonal trend (Fig. 4), we also observed one very negative $\Delta^{14}C$ signature (−223‰ on 9/22/07). This sample also had a typical "marine" stable isotopic and elemental composition similar to other HMW DOM samples ($\delta^{13}C = -21.3‰$, C:N ~10; Walker and McCarthy, 2012), providing no obvious explanation for the extreme $\Delta^{14}C$ value. One possibility is that this sample reflects the influence of internal waves on the central CA coast bringing deeper DOM to the surface, consistent with the large change in SST during this sample period (SST warming from 11.7 to 14.5 °C; September 21–25, 2007), or potentially the introduction of offshore DOM via a mesoscale eddy. Both of these processes have been shown to strongly affect both thermocline depth and DOM concentrations (e.g. Bray and Greengrove, 1993; Letelier et al., 2000). However, in the open Pacific ocean, HMW DOM with $\Delta^{14}C$ values in this range (−200‰ to −300‰) are typically found only at mesopelagic depths (600–2000 m; Walker et al., 2011) – suggesting that this is not a likely explanation. Nevertheless, all other HMW DOM samples measured during the study period have the $\Delta^{14}C$ signatures within expected variability for surface HMW DOM from the Pacific ocean (Walker et al., 2011), consistent with stable isotopic and elemental ratios (Walker and McCarthy, 2012).

The most negative HMW DOM $\Delta^{14}C$ values occurred during either the winter "Davidson" and spring/summer "Upwelling" CCS periods (average $\Delta^{14}C = -119 \pm 32‰$, $n = 4$), while the higher HMW DOM $\Delta^{14}C$ values were observed during the late summer "Oceanic" CCS periods ($\Delta^{14}C = -15 \pm 19‰$, $n = 6$; excluding the 9/22/07 sample). The similarity between HMW DOM and DIC $\Delta^{14}C$ during the Oceanic periods in both 2007 and 2008 (Fig. 4), coupled with previous observations of significant C-rich DOM production (Walker and McCarthy, 2012), strongly suggests that recently produced carbohydrates dominate during periods of water column stratification and higher SST, consistent with expectations from DOM studies in the open ocean (Goldberg et al., 2009). In contrast, low HMW DOM $\Delta^{14}C$ values from the Davidson and Upwelling periods (Fig. 4) suggest that the upwelling of ^{14}C-depleted DOM contributes significantly to the $\Delta^{14}C$ signature of HMW DOM. This offset between DIC $\Delta^{14}C$ and HMW DOM is also consistent with the unique "HNLC" character (i.e. low DOM and POM production/export during spring upwelling; Walker and McCarthy, 2012) of the Big Sur coast – suggesting that "older" HMW DOM is predominant during upwelling periods.

A Keeling plot of 1/HMW DOC and $\Delta^{14}C$ confirms this basic idea and indicates that seasonal HMW DOM $\Delta^{14}C$ patterns in this upwelling center can be largely explained by two-component mixing (Fig. 5; $R^2 = 0.66$, $p = 0.0042$). Here the production of C-rich HMW DOM in the late summer "Oceanic" CCS periods have modern $\Delta^{14}C$ signatures and adhere strictly to the mixing line, whereas N-rich HMW DOM (Walker and McCarthy, 2012) produced during Upwelling and "Davidson" periods have lower $\Delta^{14}C$ values that also deviate from the mixing line (e.g. at $1/[DOC] = 0.2$). A Keeling intercept of $\Delta^{14}C = +88 \pm 33‰$ suggests that the $\Delta^{14}C$ signature of 'new' HMW DOM added to this upwelling system carries an open ocean 'bomb' DIC $\Delta^{14}C$ value, slightly higher than our measured range of *in situ* DIC $\Delta^{14}C$. This is consistent with previous work suggesting that advected HMW DOM from the surface open ocean strongly influences this region during the "oceanic" CCS period (Walker and McCarthy, 2012). It should also be noted that this Keeling intercept (+88‰) is higher than surface ocean DIC $\Delta^{14}C$ values reported prior to 2006 (<+40‰; Druffel et al., 2010). Assuming Keeling model assumptions and two-component mixing are valid for this upwelling system, this may also imply that HMW DOM in the open and/or coastal ocean may persist for several years before being remineralized. Unfortunately, we do not have enough data to perform a similar analysis on HMW DOM from individual CCS periods. Such analysis would be useful for differentiating between 'new' HMW DOM production vs. 'background' HMW DOM $\Delta^{14}C$ values for each CCS period (i.e. Oceanic, Davidson, Upwelling). While these results suggest that physical mixing can be important for seasonally determining *bulk* HMW

Table 3
High molecular weight dissolved organic matter (HMW DOM): stable and radiocarbon isotopic data. Carbon isotopic data ($\delta^{13}C$ and $\Delta^{14}C$) for HMW DOM (0.1 μm–1 nm). Conventions for reporting $\delta^{13}C$ and $\Delta^{14}C$ data are as in Tables 1 and 2.

Sample date	$\delta^{13}C$ (‰)	±	CAMS #	Fm	±	$\Delta^{14}C$ (‰)	±	^{14}C age	±
09/21/03	−21.3	0.13	138821/143649	0.780	0.002	−223	2.4	2000	18
09/22/03	−20.7	0.11	138822	0.964	0.004	−36	4.0	295	35
09/23/03	−20.2	0.35	138823	0.968	0.005	−32	4.9	260	45
09/24/03	−20.9	0.30	138824/138825	0.974	0.007	−26	6.6	210	43
02/29/04	−19.8	0.12	138820/143774	0.885	0.003	−119	1.3	925	57
03/01/04	−18.8	0.56	138819	0.924	0.004	−76	4.4	635	40
05/09/04	−21.2	0.26	138817/138818	0.848	0.002	−152	2.3	1310	48
05/10/04	−19.9	0.33	138819	0.924	0.004	−76	4.4	635	40
09/12/04	−17.6	0.30	143637	1.006	0.003	−1	2.9	Modern	
09/13/04	−18.6	0.38	143773	1.019	0.003	12	3.5	>Modern	
09/22/04	−19.1	0.52	143650	0.997	0.003	−10	2.9	25	25

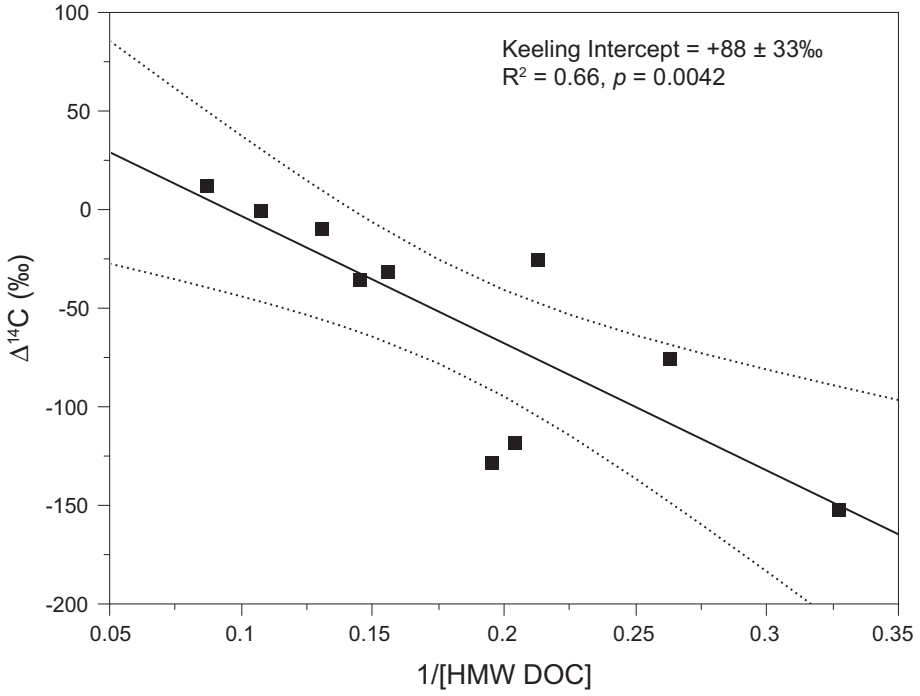

Fig. 5. High molecular weight DOM Keeling analysis. Keeling plot of inverse HMW DOC concentration (1/μM) and measured $\Delta^{14}C$ values (‰). Coefficient of determination (R^2), *p*-value and confidence limits were determined using least squares regression analysis. The Keeling *y*-intercept value and error were determined using model II geometric mean regression analysis. Thick black line and dashed lines represent the linear fit and 95% confidence limits.

DOM $\Delta^{14}C$ values, in contrast, HMW DOM isotopic signatures ($\delta^{13}C$, $\delta^{15}N$, $\Delta^{14}C$; Walker and McCarthy, 2012; this study) strongly suggest large phytoplankton cells (i.e. large POM size-fractions) are mainly responsible for overall 'new' HMW DOM produced within this upwelling system.

The seasonal production of HMW DOM with variable elemental (C:N) and isotopic ($\delta^{13}C$, $\delta^{15}N$, $\Delta^{14}C$) compositions that we observe may also have significant implications for understanding both the impact of exported DOM on offshore ecosystems, and interpreting DOM cycling within coastal margins. Previous work at this site has shown that C-rich HMW DOM is produced in late summer (C:N ~12; Walker and McCarthy, 2012). This observation is consistent with previous work examining dissolved carbohydrate production within upwelling systems (Nieto-Cid et al., 2004). If we assume that the C-rich, and modern $\Delta^{14}C$ HMW DOM seasonal production at this upwelling system is carbohydrate-dominated, then the export of this labile material may represent a significant contribution of modern C to offshore DOM pools. In contrast, the N-rich HMW and total DOM produced during upwelling (C:N $\leqslant$ 10; Walker and McCarthy, 2012) has more negative $\Delta^{14}C$ values (−75‰ to −150‰), suggesting that upwelling-derived DOM exported from this region may represent a source of labile yet "pre-aged" DOM augmenting offshore ecosystems. These variable HMW DOM $\Delta^{14}C$ signatures, together with previously observed variability in total and DOM elemental compositions from other upwelling systems (Alvarez-Salgado et al., 2001a,b; Hill and Wheeler, 2002) highlights the need to further constrain the chemical and isotopic variability of DOM from coastal regions – especially considering DOM may comprise the majority of exported labile carbon and nitrogen from upwelling systems.

3.3. Determination of upwelling-derived vs. allochthonous POM contributions

While our hypothesis of DIC $\Delta^{14}C$ incorporation into major OM pools is generally correct, there are also unexpected results in both OM ^{14}C-composition and seasonal variation. For example, from past bulk elemental and isotopic composition data (Walker and McCarthy, 2012), we expected the bulk large POM to closely track *in situ* DIC $\Delta^{14}C$, yet it did not. Overall, our results show that mixtures of newly-produced vs. "pre-aged" OM (likely derived from re-suspended marine sediments) can be found throughout the time series and in all OM pools. This suggests that in order to accurately determine the proportion of upwelled DIC ultimately exported as POM, a quantitative measure of newly fixed vs. pre-aged OM is required. Here we estimate source OM contributions to both large and small POM size-fractions using a triple isotope ($\delta^{15}N$, $\delta^{13}C$, $\Delta^{14}C$) Bayesian statistics mixing model (MixSIR; see Section 2.4).

Input values are estimated from observations in the nearby Monterey Bay Region. We note that due to a lack of observations we do not include aerosol OM $\delta^{13}C$, $\delta^{15}N$ and $\Delta^{14}C$ values which are unknown for the California coast. However, because our study site is largely free of

anthropogenic influences, marine aerosol POM is the most likely source to our measured POM pools. For our model, we consider the following major OM source contributors: (1) re-suspended sedimentary organic matter (SOM) ($\delta^{13}C = -26 \pm 2‰$, $\delta^{15}N = +2.5 \pm 2‰$, $\Delta^{14}C = -170 \pm 30‰$; Peters et al., 1978; Paull et al., 2006), (2) coastal phytoplankton ($\delta^{13}C = -22 \pm 2‰$, $\delta^{15}N = +5 \pm 2‰$, $\Delta^{14}C = +10 \pm 20‰$; Rau et al., 1998; Walker and McCarthy, 2012), (3) commonly ascribed open ocean phytoplankton values ($\delta^{13}C = -20 \pm 2‰$, $\delta^{15}N = 0 \pm 2‰$, $\Delta^{14}C = +60 \pm 5‰$) and (4) littoral/macrophyte OM ($\delta^{13}C = -17 \pm 3‰$, $\delta^{15}N = +6 \pm 3‰$, $\Delta^{14}C = +10 \pm 20‰$; ($\delta^{13}C = -17 \pm 3‰$, $\delta^{15}N = +6 \pm 3‰$, $\Delta^{14}C = +10 \pm 20‰$; Foley and Koch, 2010; this study).

Using these endmember values, we model the seasonal contribution of SOM vs. "fresh" marine production for both our large and small POM sample populations during both "upwelling" vs. "non-upwelling" periods (Fig. 6). For large and small POM sample populations, we found that the large POM pool is comprised of coastal phytoplankton OM ($83 \pm 5\%$) and that the small POM pool appears to be dominated by littoral/macrophyte OM ($77 \pm 4\%$). The model also suggests that large and small POM sample populations overall contain between 10% and 18% SOM. However, by differentiating each POM size-fraction by periods of upwelling vs. non-upwelling, the model reveals several clear differences. For example, POM collected during coastal upwelling periods contains far more SOM ($22 \pm 1\%$ and $44 \pm 4\%$ for large and small POM, respectively). We also find that coastal phytoplankton OM is in higher abundance during non-upwelling periods, consistent with previous observations of increased POC and PON abundance during stratified conditions (Walker and McCarthy, 2012). With the exception of non-upwelling small POM samples, the model predicted contributions of open ocean phytoplankton were generally small (<2%) within both large and small POM size-fractions. Overall, these results indicate that large POM is the predominant mode of exporting recently-fixed, upwelling-derived POM (coastal phytoplankton OM) from this site, with the small POM size-fraction being dominated by both SOM and littoral/macrophyte OM contributions. Also, while these mixture contributions are variable, the generally negative POM $\Delta^{14}C$ signatures we observe with respect to measured DIC $\Delta^{14}C$ are largely explained by the presence of ^{14}C-depleted SOM contributions during intense water column mixing/upwelling events. While some resuspended sediment is to be expected at nearshore upwelling sites, the influence probably scales with the width of the shelf and available sediment (fetch). We hypothesize that wide-shelf upwelling regions; such as the Davenport upwelling plume, Oregon coast, etc., could have *more* SOM contributing to large and small POM fractions.

Our estimates of SOM contributions, although realistic and well constrained, are limited by our assumptions. For example, contributions of POM sources with negative $\Delta^{14}C$ signatures would also 'mask' recently produced POM $\Delta^{14}C$ signals. In order to use DIC and POM $\Delta^{14}C$

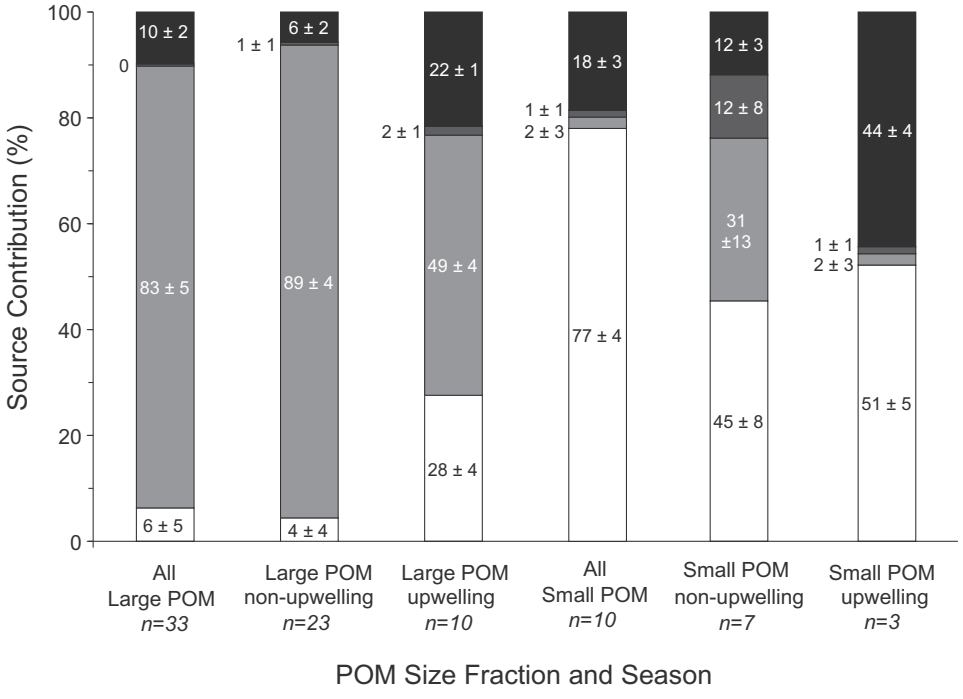

Fig. 6. Bar plot of MixSIR model allochthonous POM contributions. Allochthonous POM contributions to large and small POM are shown as a bar plot as derived by the MixSIR model (see Section 2.4). Black, dark grey, light grey and white regions represent sedimentary, open ocean phytoplankton, coastal phytoplankton and littoral/macrophyte POM contributions, respectively. Errors on relative percent contribution estimates were derived using model calculated interquartile ranges (IQR) of contribution distributions using the relationship: standard deviation = IQR/1.35.

signatures to more precisely quantify upwelling-derived OM production and export from coastal margins, it is likely that direct $\Delta^{14}C$ measurements of labile vs. pre-aged OM pools will be required. Future work should focus on methods to geochemically isolate "newly-produced" vs. "pre-existing" POM components. Recent work suggests that simple hydrolytic-based organic separations of marine POM can accomplish this function (e.g. total lipid extraction coupled with acid-soluble and acid-insoluble chemical fractionation; Wang et al., 1998; Hwang and Druffel, 2006; Hwang et al., 2006; Roland et al., 2008). Here, $\delta^{13}C$ and $\Delta^{14}C$ signatures of total lipid and non-hydrolysable "acid-insoluble" components comprise refractory materials (e.g. resuspended sedimentary OM and terrestrial sources), while hydrolysable or "acid-soluble" POM represents almost exclusively newly-produced labile OM. We hypothesize that a similar approach could be used to isolate fresh (primary production) vs. re-suspended sedimentary contributions within the POM pool – yielding more precise estimates of upwelling-derived OM production/export from coastal margins.

3.4. Size–age–composition relationships of major organic matter pools

The physical size of OM is strongly linked to its bioavailability; an idea typically referred to as the "size–reactivity continuum" hypothesis (Amon and Benner, 1996). Relative molecular size is therefore thought to play a key role in the relative fate and lability of detrital OM (i.e. containing the lowest C:N ratios, abundance of "fresh" biomolecules and highly-positive $\Delta^{14}C$ signatures; Druffel et al., 1992; Guo et al., 1996; Benner and Kaiser, 2003; Loh et al., 2004; Kaiser and Benner, 2009). However, bioavailability is not always synonymous with $\Delta^{14}C$ and C:N ratio, and to what degree molecular size may correlate with these parameters is far less certain. Recently, Walker et al. (2011) showed that within the oligotrophic open ocean DOM pool, relative molecular size and $\Delta^{14}C$ are strongly linked. Few qualitative observations of a size–age relationships have included POM samples (Guo et al., 1996), and quantitative relationships between OM size and $\Delta^{14}C$ has never been directly tested for any ocean region. Because OM transport (sinking vs. advection, as well as relative sinking rate) is largely affected by physical size, a strong relationship between OM size and $\Delta^{14}C$ might indicate the importance of this mechanistic process and the transport of modern vs. older carbon from coastal margins. At the same time, the diversity of possible carbon sources yielding an admixed signal might complicate observations of a direct size–$\Delta^{14}C$ relationship.

We observe statistically significant correlations between average OM size, $\Delta^{14}C$ and C:N molar ratio (Fig. 7A/B). In both Fig. 7A/B, the 95% confidence interval (CI) of slopes determined by least squares regression analysis exclude zero (95% CIs for Fig. 7A = 2.12, 8.16 and Fig. 7B = −0.7, −0.4). Thus, while coefficients of determination are low ($R^2 = 0.18$ and 0.35 for A and B, respectively), OM size vs. $\Delta^{14}C$ and C:N relationships are statistically significant. Resulting *y*-intercepts from these regressions fall

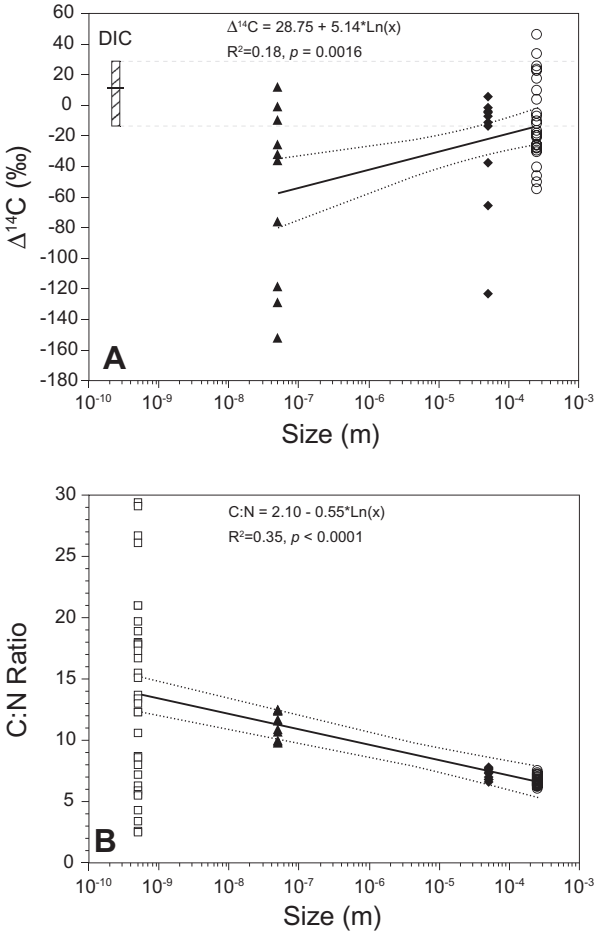

Fig. 7. Size–age–composition relationships for dissolved and particulate coastal organic matter pools. Open squares, solid triangles, solid diamonds and open circles depict total DOM, HMW DOM, Small and Large POM organic matter size fractions. (A) Radiocarbon $\Delta^{14}C$ values (*y*) are shown in the context of organic matter size (*x*). Crosshatched rectangle and dashed horizontal lines represent the total range in measured DIC $\Delta^{14}C$ values during the time series, and the horizontal black bar represents the average DIC $\Delta^{14}C$ value ($n = 30$). (B) Elemental (C:N molar ratios) data (*y*) are shown in the context of organic matter size (*x*). Raw data for this figure was adapted from Walker and McCarthy (2012). For both A and B, size (*x*) values correspond to the mid-point of pre/filter size cutoffs for HMW DOM (1 nm–0.1 μm), large POM (0.7–500 μm) and small POM (0.1–100 μm) fractions (e.g. equal biomass C per size interval; Sheldon et al., 1972; Chisholm, 1992). In the case of total DOM, a size (*x*) value of 5×10^{-10} m (or ~500 Da) was used given ~70–80% of DOC is considered smaller than ~1 nm. Thick black and dashed lines depict the least squares regressions and 95% confidence intervals determined using JMP v10.

within our measured DIC $\Delta^{14}C$ range (Fig. 7A: $\Delta^{14}C = 28 \pm 16‰$) and a C:N ratio (Fig. 7B: C:N = 2.1 ± 1.2) closely approximating that of fresh, proteinaceous material. These *y*-intercepts further reinforce the idea that prior to degradation, recently produced OM is chemically 'fresh' and has a $\Delta^{14}C$ signature similar to that of surface DIC. Preliminary results from $\Delta^{14}C$ analysis of the total DOM pool suggest that size vs. $\Delta^{14}C$ correlations

improve further when these measurements are included ($R^2 = 0.83$; Walker unpublished data) – suggesting size vs. $\Delta^{14}C$ relationships may be much stronger within this upwelling system.

The presence of size vs. $\Delta^{14}C$ and C:N relationships are somewhat surprising given: (1) the dynamic cycling of dissolved vs. particulate OM pools, (2) strong inter-seasonal variability of physical and biological processes (Walker and McCarthy, 2012) and (3) impact of "pre-aged" OM sources. To our knowledge, this is the first observation of *quantitative* relationships between bulk chemical composition, $\Delta^{14}C$, and marine OM size, perhaps representing a significant expansion on size–reactivity continuum ideas (e.g. Amon and Benner, 1994; Kaiser and Benner, 2009). We do not, however, observe a direct or 'instantaneous' correlation between sample OM $\Delta^{14}C$ values and C:N ratios ($R^2 = 0.06$; not shown). This suggests that OM aging and compositional changes operate on very different timescales, and that dynamic physical and biological processes preclude contemporaneous $\Delta^{14}C$ vs. C:N relationships. The C:N ratio of marine DOM can be largely affected by periods of intense carbohydrate production on short timescales in the surface ocean (C:N ~19–25; Biersmith and Benner, 1998) and gradual removal of nitrogenous DOM in the deep ocean over long timescales (Benner et al., 1992, 1997). At this coastal site in particular, we find periods of intense inter-seasonal DOC and DON production (Walker and McCarthy, 2012). Only when all time series data are considered do we begin to observe quantitative size–age–continuum relationships.

These basic $\Delta^{14}C$ and C:N vs. size relationships might also have implications for understanding linkages between DOM vs. POM at coastal margins. The trends we observe suggest a flow of OM from modern (and chemically "fresh") large POM, to smaller POM and finally into the DOM pool. This is broadly consistent with previous $\Delta^{14}C$ observations of DOM and POM from the Gulf of Mexico (Guo et al., 1996). Given previous work showing that molecular size and composition of DOM strongly determine its $\Delta^{14}C$ signature (e.g. Walker et al., 2011), we hypothesize that when considering large sample populations and size-fractions, this trend may continue throughout the DOM size–age–composition continuum – from large, chemically "fresh" DOM macromolecules with modern ^{14}C-ages to smaller, more degraded DOM molecules with older ^{14}C-ages.

Such relationships may also represent a framework for testing DOM/POM transformation mechanisms in the ocean. For example, previous work has shown that marine gels (e.g. self-assembled gels (SAG) and transparent exopolymer particles (TEP); Chin et al., 1998; Verdugo et al., 2004) can represent a "bridge" of OM exchange between the DOM/POM pools. While, the size–age–composition continuum we observe in this upwelling system seems to rule out gel formation (i.e. production of C-rich, "old" macromolecules from existing DOM) as a quantitatively important process, it is possible that in microbial-dominated oligotrophic systems this may not be the case. If DOM and POM size-classes do not have robust size–age–composition relationships (i.e. C:N ratios and $\Delta^{14}C$ values that deviate from the trendline) in other ocean regions, this might be more consistent with SAG or TEP formation. Such an outcome would suggest that DOM/POM linkages are more complicated, perhaps involving multiple POM/DOM transformation mechanisms (e.g., particle dis/aggregation, organic–mineral interactions, non-selective POM preservation and the incorporation of sedimentary organic carbon and/or black carbon to DOM and POM pools (e.g. Arnosti, 2004; Lee et al., 2004; Roland et al., 2008).

Overall, more work is clearly needed to assess the elemental and isotopic composition of SAG and TEP, and its possible role in a DOM/POM size–age–composition continuum. In particular, the $\Delta^{14}C$ signature of marine gels remains completely unknown. Our data suggest a number of testable hypotheses. Given the size–age–composition trends we observe, we would predict that SAG/TEP sampled within this upwelling system should have $\Delta^{14}C$ signatures between that of our small POM and HMW DOM size-fractions (or $\Delta^{14}C \sim -20‰$ to $-60‰$). These predicted $\Delta^{14}C$ values for microgel DOM fractions are strongly ^{14}C-enriched in comparison to surface DOM from the open ocean ($\Delta^{14}C$ ~250‰; Walker et al., 2011), suggesting that if marine microgels are exported, they may represent highly labile DOM, possibly augmenting offshore ecosystems. Similarly, an open ocean size–age–composition continuum would predict that the $\Delta^{14}C$ signature of marine microgels also be ^{14}C-enriched. If instead SAG/TEP does not follow size vs. $\Delta^{14}C$ trends, this would then imply the discrete cycling of marine gels from both DOM and POM pools.

4. CONCLUSIONS

This study is the first to characterize the contemporaneous $\Delta^{14}C$ signature of DIC, HMW DOM, and size-fractionated POM. One major goal was to assess if the direct incorporation of an upwelled DIC $\Delta^{14}C$ signal may represent a new, direct tracer for upwelling-derived OM production and export from upwelling regions. Our results show that upwelling has a strong and predictable effect on DIC $\Delta^{14}C$ signatures within this upwelling system. Despite the attenuation of the bomb ^{14}C-signal, we observe a large seasonal DIC $\Delta^{14}C$ signal (>40‰), which is also incorporated into both POM and HMW DOM pools. Together, these observations indicate that $\Delta^{14}C$ values can be used as a viable direct tracer of upwelled inorganic carbon incorporation into new and exported production. However, pre-existing (^{14}C-depleted) geochemical mixtures also influenced the $\Delta^{14}C$ signature of both DOM and POM. Using a triple isotope ($\delta^{13}C$, $\delta^{15}N$, $\Delta^{14}C$) mixing model, we estimate that during periods of coastal upwelling, re-suspended sediments may contribute between 22% and 44% of "pre-aged" OM to large and small POM pools, respectively. Finally, OM size–age–composition relationships we observe within this upwelling system are a novel result. This size–age–composition trend represents the first indication that OM physical size can be quantitatively linked to both C:N ratio and $\Delta^{14}C$ – expanding upon "size–reactivity" continuum ideas. If size–age–composition relationships are widespread they may represent a new tool for modeling ocean C and N biogeochemical cycles.

ACKNOWLEDGEMENTS

We gratefully acknowledge Bryn Phillips, Katie Seigler and the staff of the Granite Canyon Marine Pollution Studies Laboratory (GCMPSL) for providing facilities capable of biweekly and large-volume seawater DOM and suspended POM isolations. Jennifer Lehman, Leslie Roland, Kona Walker, Gemma Vila Reixach, and Maria Calleja (UC Santa Cruz) for help with fieldwork and sample collection. Dyke Andreasen of the UC Santa Cruz Stable Isotope Laboratory for help with CHN and stable isotopic analysis. We also thank three anonymous reviewers for their insightful comments. This work was funded by the Friends of Long Marine Lab Student Research Awards (to B.D.W.), the UC Santa Cruz STEPS Institute for Innovation in Environmental Research (to B.D.W.), the UC Santa Cruz Center for the Dynamics and Evolution of the Land-Sea Interface (to B.D.W.), the Earl H. Myers and Ethel M. Myers Oceanographic and Marine Biology Trust (to B.D.W.), and the UC Santa Cruz Institute of Geophysics and Planetary Physics (to B.D.W. and M.D.M.). A portion of this work was performed under the auspices of the U.S. Department of Energy (contract W-7405-Eng-48 and DE-AC52-07NA27344).

REFERENCES

Alvarez-Salgado X. A., Doval M. D., Borges A. V., Joint I., Frankignoulle M., Woodward E. M. S. and Figueiras F. G. (2001a) Off-shelf fluxes of labile materials by an upwelling filament in the NW Iberian upwelling system. *Prog. Oceanogr.* **51**, 321–337.

Alvarez-Salgado X. A., Gago J., Miguez B. M. and Perez F. F. (2001b) Net ecosystem production of dissolved organic carbon in a coastal upwelling system: the Ria de Vigo, Iberian margin of the North Atlantic. *Limnol. Oceanogr.* **46**, 135–147.

Amon R. M. W. and Benner R. (1994) Rapid cycling of high molecular weight dissolved organic matter in the ocean. *Nature* **369**, 549–552.

Amon R. M. W. and Benner R. (1996) Bacterial utilization of different size classes of dissolved organic matter. *Limnol. Oceanogr.* **41**, 41–51.

Arnosti C. (2004) Speed bumps and barricades in the carbon cycle: substrate structural effects on carbon cycling. *Mar. Chem.* **92**, 263–273.

Bakun, A. (1973) Coastal upwelling indices west coast of North America 1946–1971. NOAA (National Oceanic and Atmospheric Administration) Technical Report NMFS (National Marine Fisheries Service) SSRF (Special Scientific Report Fisheries) **671**, pp. 1–103.

Barth J., Cowles T., Kosro P., Shearman R., Huyer A. and Smith R. L. (2002) Injection of carbon from the shelf to offshore beneath the euphotic zone in the California Current. *J. Geosphys. Res. Oceans.* **107**. Art. No. 3057.

Bauer J. E. and Druffel E. R. M. (1998) Ocean margins as a significant source of organic matter to the deep open ocean. *Nature* **392**, 482–485.

Benner R. and Kaiser K. (2003) Abundance of amino sugars and peptidoglycan in marine particulate and dissolved organic matter. *Limnol. Oceanogr.* **48**, 118–128.

Benner R., Pakulski J. D., McCarthy M., Hedges J. I. and Hatcher P. G. (1992) Bulk chemical characteristics of dissolved organic matter in the ocean. *Science* **255**, 1561–1564.

Benner R., Biddanda B., Black B. and McCarthy M. (1997) Abundance, size distribution, and stable carbon and nitrogen isotopic compositions of marine organic matter isolated by tangential-flow ultrafiltration. *Mar. Chem.* **57**, 243–263.

Biersmith A. and Benner R. (1998) Carbohydrates in phytoplankton and freshly produced dissolved organic matter. *Mar. Chem.* **63**, 131–144.

Biller D. B., Coale T. H., Till R. C., Smith G. J. and Bruland K. W. (2013) Coastal iron and nitrate distributions during the spring and summer upwelling season in the central California Current upwelling regime. *Cont. Shelf Res.* **66**, 58–72.

Bray N. A. and Greengrove C. L. (1993) Circulation over the shelf and slope off Northern California. *J. Geophys. Res.* **98**, 18119–18145.

Breaker L. C. (2005) What's happening in Monterey Bay on seasonal to interdecadal time scales. *Cont. Shelf Res.* **25**, 1159–1193.

Bruland K. W., Rue E. L. and Smith G. J. (2001) Iron and macronutrients in California coastal upwelling regimes: implications for diatom blooms. *Limnol. Oceanogr.* **46**, 1661–1674.

Cassar N., Laws E. A., Bidigare R. R. and Popp B. N. (2004) Bicarbonate uptake by Southern Ocean phytoplankton. *Global Biogeochem. Cycles*, 18.

Chavez F. P. A. T. R. J. (1995) *Physical Estimates of Global New Production: The Upwelling Contribution*. John Wiley, Hoboken, NJ.

Chin W. C., Orellana M. V. and Verdugo P. (1998) Spontaneous assembly of marine dissolved organic matter into polymer gels. *Nature* **391**, 568–572.

Chisholm S. W. (1992) Phytoplankton size. In *Primary Productivity and Biogeochemical Cycles in the Sea* (eds. P. G. Falkowski and A. D. Woodhead). Plenum Press, New York.

Collins C. A., Pennington J. T. and Castro C. G., et al. (2003) The California Current system off Monterey, California: physical and biological coupling. *Deep-Sea Res.* **50**, 2389–2404.

Druffel E. R. M., Williams P. M., Bauer J. E. and Ertel J. R. (1992) Cycling of dissolved and particulate organic matter in the open ocean. *J. Geophys. Res.* **97**, 15639–15659.

Druffel E. R. M., Bauer J. E. and Williams P. M., et al. (1996) Seasonal variability of particulate organic radiocarbon in the northeast Pacific Ocean. *J. Geophys. Res.* **101 C9**, 20543–20552.

Druffel E. R. M., Beaupre S., Griffin S. and Hwang J. (2010) Variability of dissolved inorganic radiocarbon at a surface site in the Northeast Pacific Ocean. *Radiocarbon* **52**, 1150–1157.

Fassbender A. J., Sabine C. L., Feely R. A., Langdon C. and Mordy C. W. (2011) Inorganic carbon dynamics during northern California coastal upwelling. *Cont. Shelf Res.* **31**, 1180–1192.

Foley M. M. and Koch P. L. (2010) Correlation between allochthonous subsidy input and isotopic variability in the giant kelp Macrocystis pyrifera in central California, USA. *Mar. Ecol. Prog. Ser.* **409**, 41–50.

Fry B., Brand W., Mersch F. J., Tholke K. and Garritt R. (1992) Automated-analysis system for coupled delta C-13 and deltat N-15 measurements. *Anal. Chem.* **64**, 288–291.

Goldberg S. J., Carlson C. A., Hansell D. A., Nelson N. B. and Siegel D. A. (2009) Temporal dynamics of dissolved combined neutral sugars and the quality of dissolved organic matter in the Northwestern Sargasso Sea. *Deep-Sea Res.* **56**, 672–685.

Gruber N., Frenzel H., Nagai T., Leinweber A., Plattner G., McWilliams J. C., Stolzenbach K. D., Chavez F., Friederich G., Hales B. and Doney S. C. (2006) Toward a first carbon budget for the U.S. West Coast's margins. *EOS Trans. Am. Geophys. Union* **87**, Ocean Sci. Meet. Suppl. Abstract OS33D-04.

Guo L. D., Santschi P. H., Cifuentes L. A., Trumbore S. E. and Southon J. (1996) Cycling of high-molecular-weight dissolved organic matter in the middle Atlantic bight as revealed by carbon isotopic (C-13 and C-14) signatures. *Limnol. Oceanogr.* **41**, 1242–1252.

Hales B., Takahashi T. and Bandstra L. (2005) Atmospheric CO2 uptake by a coastal upwelling system. *Global Biogeochem. Cycles*, 19.

Hill J. K. and Wheeler P. A. (2002) Organic carbon and nitrogen in the northern California current system: comparison of offshore, river plume, and coastally upwelled waters. *Prog. Oceanogr.* **53**, 369–387.

Hinger E. N., Santos G. M., Druffel E. R. M. and Griffin S. (2010) Carbon isotope measurements of surface seawater from a time-series site off Southern California. *Radiocarbon* **52**, 69–89.

Hutchins D. A. and Bruland K. W. (1998) Iron-limited diatom growth and Si:N uptake ratios in a coastal upwelling regime. *Nature* **393**, 561–564.

Hutchins D. A., DiTullio G. R., Zhang Y. and Bruland K. W. (1998) An iron limitation mosaic in the California upwelling regime. *Limnol. Oceanogr.* **43**, 1037–1054.

Hwang J. and Druffel E. R. M. (2006) Carbon isotope ratios of organic compound fractions in oceanic suspended particles. *Geophys. Res. Lett.*, 33.

Hwang J., Druffel E. R. M., Eglinton T. I. and Repeta D. J. (2006) Source(s) and cycling of the nonhydrolyzable organic fraction of oceanic particles. *Geochim. Cosmochim. Acta* **70**, 5162–5168.

Kaiser K. and Benner R. (2009) Biochemical composition and size distribution of organic matter at the Pacific and Atlantic time-series stations. *Mar. Chem.* **113**, 63–77.

Key R. M., Quay P. D., Jones G. A., McNichol A. P., vonReden K. F. and Schneider R. J. (1996) WOCE AMS radiocarbon.1. Pacific Ocean results (P6, P16 and P17). *Radiocarbon* **38**, 425–518.

Laws E. A., Popp B. N., Cassar N. and Tanimoto J. (2002) C-13 discrimination patterns in oceanic phytoplankton: likely influence of CO2 concentrating mechanisms, and implications for palaeoreconstructions. *Funct. Plant Biol.* **29**, 323–333.

Lee C., Wakeham S. and Arnosti C. (2004) Particulate organic matter in the sea: the composition conundrum. *Ambio* **33**, 565–575.

Letelier R. M., Karl D. M., Abbott M. R., Flament P., Freilich M., Lukas R. and Strub T. (2000) Role of late winter mesoscale events in the biogeochemical variability of the upper water column of the North Pacific Subtropical Gyre. *J. Geophys. Res.* **105**, 28723–28739.

Loh A. N., Bauer J. E. and Druffel E. R. M. (2004) Variable ageing and storage of dissolved organic components in the open ocean. *Nature* **430**, 877–881.

Mahadevan A. (2001) An analysis of bomb radiocarbon trends in the Pacific. *Mar. Chem.* **73**, 273–290.

Masiello C. A., Druffel E. R. M. and Bauer J. E. (1998) Physical controls on dissolved inorganic radiocarbon variability in the California Current. *Deep-Sea Res.* **45**, 617–642.

McNichol A. P. and Aluwihare L. I. (2007) The power of radiocarbon in biogeochemical studies of the marine carbon cycle: insights from studies of dissolved and particulate organic carbon (DOC and POC). *Chem. Rev.* **107**, 443–466.

McNichol A. P., Jones G. A., Hutton D. L., Gagnon A. R. and Key R. M. (1994) The Rapid Preparation of Seawater ΣCO_2 for Radiocarbon Analysis at the National Ocean Sciences AMS Facility. *Radiocarbon* **36**, 237–246.

Moore J. W. and Semmens B. X. (2008) Incorporating uncertainty and prior information into stable isotope mixing models. *Ecol. Lett.* **11**, 470–480.

Muller-Karger F. E., Varela R., Thunell R., Luerssen R., Hu C. M. and Walsh J. J. (2005) The importance of continental margins in the global carbon cycle. *Geophys. Res. Lett.*, 32.

Nieto-Cid M., Alvarez-Salgado X. A., Brea S. and Perez F. F. (2004) Cycling of dissolved and particulate carbohydrates in a coastal upwelling system (NW Iberian Peninsula). *Mar. Ecol. Prog. Ser.* **283**, 39–54.

Paull C. K., Ussler W., Mitts P. J., Caress D. W. and West J. G. (2006) Discordant 14C-stratigraphies in upper Monterey Canyon: a signal of anthropogenic disturbance. *Mar. Geol.* **223**, 21–36.

Pennington J. T., Friederich G. E., Castro C. G., Collins C. A., Evans W. W. and Chavez F. P. (2010) The northern and central California coastal upwelling system. In *Carbon and Nutrient Fluxes in Continental Margins: A Global Synthesis* (eds. K. K. Liu, L. Atkinson, R. Quinones and L. Talaue-McManus), 1st ed. Springer-Verlag, Berlin Heidelberg, p. 744.

Peters K. E., Sweeney R. E. and Kaplan I. R. (1978) Correlation of carbon and nitrogen stable isotope ratios in sedimentary organic matter. *Limnol. Oceanogr.* **23**, 598–604.

Rau G. H., Takahashi T. and Marais D. J. D. (1989) Latitudinal variations in plankton delta C-13 – implications for CO2 and productivity in past oceans. *Nature* **341**, 516–518.

Rau G., Low C., Chavez F. and Friederich G. E. (1997a) The relationship between del13C-DIC and pCO2 dynamics in Monterey Bay California. *Trans. Am. Geophys. Union*, 78.

Rau G. H., Riebesell U. and WolfGladrow D. (1997b) CO2aq-dependent photosynthetic C-13 fractionation in the ocean: A model versus measurements. *Global Biogeochem. Cycles* **11**, 267–278.

Rau G. H., Low C., Pennington J. T., Buck K. R. and Chavez F. P. (1998) Suspended particulate nitrogen delta N-15 versus nitrate utilization: observations in Monterey Bay, CA. *Deep-Sea Res.* **45**, 1603–1616.

Rau G. H., Chavez F. P. and Friederich G. E. (2001a) Plankton C-13/C-12 variations in Monterey Bay, California: evidence of non-diffusive inorganic carbon uptake by phytoplankton in an upwelling environment. *Deep-Sea Res.* **48**, 79–94.

Rau G. H., Ralston S., Southon J. R. and Chavez F. P. (2001b) Upwelling and the condition and diet of juvenile rockfish: A study using C-14, C-13, and N-15 natural abundances. *Limnol. Oceanogr.* **46**, 1565–1570.

Robinson S. W. (1981) Natural and man-made radiocarbon as a tracer for coastal upwelling processes. In *Coastal Upwelling* (ed. F. A. Richards). American Geophysical Union, Washington, DC, pp. 298–302.

Roland L. A., McCarthy M. D. and Guilderson T. (2008) Sources of molecularly uncharacterized organic carbon in sinking particles from three ocean basins: a coupled delta C-14 and delta C-13 approach. *Mar. Chem.* **111**, 199–213.

Roland L. A., McCarthy M. D., Peterson T. D. and Walker B. D. (2009) A large-volume micro-filtration system for isolating suspended particulate organic matter: fabrication and assessment vs. GFF filters in central N. Pacific. *Limnol. Oceanogr.* **7**, 64–80.

Santos G. M., Ferguson J., Acaylar K., Johnson K. R., Griffin S. and Druffel E. (2011) Deta C-14 and delta C-13 of seawater DIC as tracers of coastal upwelling: a 5-year time series from Southern California. *Radiocarbon* **53**, 669–677.

Sheldon R. W., Sutcliff W. H. and Prakash A. (1972) Size distribution of particles in the ocean. *Limnol. Oceanogr.* **17**, 327.

Stuiver M. and Polach H. A. (1977) Discussion: reporting of 14C data. *Radiocarbon* **19**, 355–363.

Torres M. E., Mix A. C. and Rugh W. D. (2005) Precise delta C-13 analysis of dissolved inorganic carbon in natural waters using automated headspace sampling and continuous-flow mass spectrometry. *Limnol. Oceanogr.* **3**, 349–360.

Tortell P. D., Rau G. H. and Morel F. M. M. (2000) Inorganic carbon acquisition in coastal Pacific phytoplankton communities. *Limnol. Oceanogr.* **45**, 1485–1500.

Verdugo P., Alldredge A. L., Azam F., Kirchman D. L., Passow U. and Santschi P. H. (2004) The oceanic gel phase: a bridge in the DOM-POM continuum. *Mar. Chem.* **92**, 67–85.

Vogel J. S., Southon J. R. and Nelson D. E. (1987) Catalyst and binder effects in the use of filamentous graphite for Ams. *Nucl. Instrum. Methods B* **29**, 50–56.

Walker B. D. and McCarthy M. (2012) Elemental and isotopic characterization of dissolved and particulate organic matter in a unique California upwelling system: importance of size and composition in the export of labile material. *Limnol. Oceanogr.* **57**, 1757–1774.

Walker B. D., Beaupre S. R., Guilderson T. P., Druffel E. R. M. and McCarthy M. D. (2011) Large-volume ultrafiltration for the study of radiocarbon signatures and size vs. age relationships in marine dissolved organic matter. *Geochim. Cosmochim. Acta* **75**, 5187–5202.

Wang X. C., Druffel E. R. M., Griffin S., Lee C. and Kashgarian M. (1998) Radiocarbon studies of organic compound classes in plankton and sediment of the northeastern Pacific Ocean. *Geochim. Cosmochim. Acta* **62**, 1365–1378.

Associate editor: Andrew Ross Bowie